All-Weld-Metal Design for AWS E10018M, E11018M and E12018M Type Electrodes

The best combination of alloying elements to provide optimum toughness and strength is investigated

BY E. S. SURIAN AND L. A. de VEDIA

ABSTRACT. This paper presents the results of a research program conducted to design the all-weld metal deposited with AWS A5.5-81[1] E10018M[2], E11018M[2] and E12018M[2] SMAW-type electrodes. The role that different alloying elements such as manganese, carbon and chromium play on the tensile properties, hardness and toughness as well as on the microstructure was studied. Criteria for selecting the weld metal composition leading to optimum combination of tensile strength and toughness are suggested. The effect of the variation of heat input, within the requirements of the AWS standard, on the mentioned properties was also analyzed. It was found that the E11018M and E12018M all-weld-metal tensile properties are very sensitive to variations in heat input. For certain values of chemical composition, welding parameter ranges suitable to guarantee the fulfillment of AWS requirements were determined.

Introduction

In recent years there has been an increased use of medium- and high-strength structural steels, posing a need for adequate welding consumables for such materials. This led to a significant advance in electrode formulation to obtain weld deposits with high values for strength and good toughness (Ref. 3). Structural safety and a tolerance for discontinuities in welded joints are obtained by imposing requirements on toughness by setting minimum Charpy V-notch levels at an arbitrary temperature, and minimum CTOD values at the lowest design temperature (Ref. 4). The achievement of adequate CTOD values becomes increasingly difficult as the weld metal tensile strength increases. One way to obtain improved weld metal toughness is through microstructural control, which requires taking into account the weld metal chemistry. It is generally accepted that acicular ferrite is the optimum microstructure for the as-welded C-Mn weld metal, leading to an adequate combination of strength and fracture toughness at low temperature (Refs. 5,6). Acicular ferrite has a very fine grain size and a high concentration of dislocations that are responsible for its toughness and ductility (Ref. 7). Several workers have reported that a low transition temperature can be obtained in a C-Mn weld deposit provided the proportion of acicular ferrite is maintained at a high level, and if the amount of grain boundary ferrite with aligned M-A-C is sufficiently low (Refs. 3, 4, 7, 8).

Although the influence of Mn on mechanical properties and microstructure of C-Mn weld metal is fairly well understood (Refs. 9,10), knowledge on the effects of variations in the Mn level of alloyed weld deposits is not adequate. In relation to this, the role played by different alloying elements is fairly complex. For instance, carbon behaves differently if acting alone or in the presence of other elements such as manganese, silicon or oxygen (Ref. 11). From the point of view of the influence on the microstructure of deposited weld metal (Ref. 12), an increase in the carbon content of C-Mn weld metal produces an increase in the amount of acicular ferrite at the expense of grain boundary ferrite. With reference to notch toughness, increasing the carbon of weld deposits results in a change in shape of the transition Charpy-V curves, reducing the energy level of the upper shelf and extending the transition temperature range between brittle and ductile fracture modes.

KEY WORDS

Charpy V-Notch
Toughness
High-Strength Electrode
Covered Electrodes
CTOD
Acicular Ferrite
Microstructure

E. S. SURIAN is with Universidad Tecnológica Nacional, Facultad Regional San Nicolás, DEYTEMA, Buenos Aires, Argentina. L. A. de VEDIA is with Instituto de Tecnología Prof. Jorge A. Sábato (Universidad Nacional de San Martín-CNEA), Buenos Aires, Argentina.

1. *It must be noted that this paper reviews experimental work performed between 1987 and 1996, according to AWS A5.5-81 (Ref. 1), which was later revised as A5.5-96 (Ref. 2). This is a relevant point since in the 1996 version the joint preparation was changed from the 1981 design (45-deg included angle and ½-in. [12.7-mm] root opening) to a 20-deg included angle and ⅝-in. (16-mm) root opening. As this is an important modification related to the study of the influence of variation in heat input, it would not be correct to state that the results can be extrapolated to the new test specimen design. See Conclusions.*
2. *Previously designated by AWS A5.1-81 as E10018-M, E11018-M and E12018-M.*

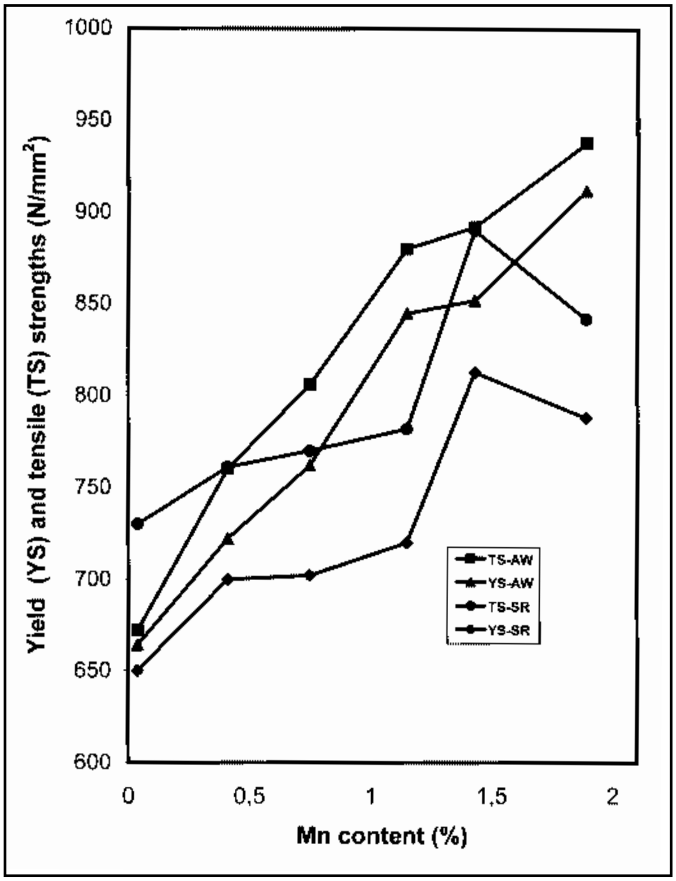

Fig. 1 — Tensile properties vs. all-weld-metal Mn content, ISO test specimens (AW, as-welded; SR, stress relieved).

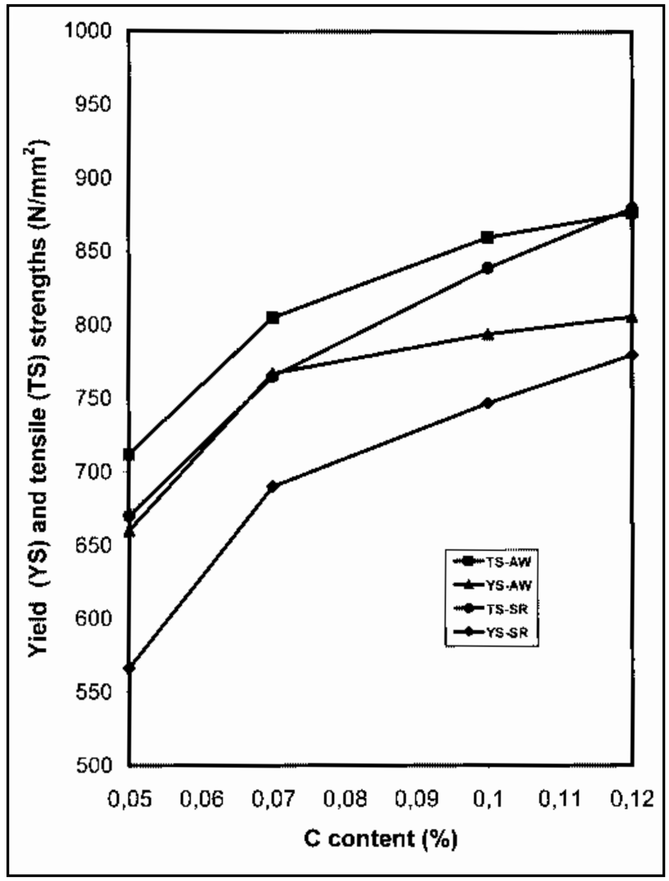

Fig. 2 — Tensile properties vs. all-weld-metal C content, ISO test specimens (AW, as-welded; SR, stress relieved).

The purpose of this work is to summarize the results of a research project conducted to develop AWS E10018M, E11018M and E12018M type electrodes suitable to deposit weld metal with optimum mechanical properties. This study consisted of an analysis of the effects of variations in the level of all-weld-metal Mn (Ref. 13), C (Ref. 14) and Cr (Refs. 15 and 16) contents on the mechanical properties and microstructure of the weld metal. Finally, using the optimum chemical composition obtained for each electrode, a study was conducted on the influence of variations of heat input (Refs. 17,18) within the range allowed by the AWS standard (Ref. 1) on the microstructure and mechanical properties of the weld metal.

Experimental Procedure

Variation of Chemical Composition of Weld Metal at Constant Heat Input

Electrodes

Six experimental iron powder basic covered electrodes that provided Mn levels in the weld metal ranging from 0.6% to 2.0% (chemical compositions are ex-

Table 1 — Welding Parameters Used in ISO 2560 Test Specimens and Single V-Groove Joints for CTOD Tests (Refs. 13, 14 and 15)

Coupon Test	Pass	Preheat and Interpass T (°C)	Amperage (A)	Voltage (V)	Heat Input (kJ/mm)
ISO all weld metal	all	93 to 107	170	24	2.1
Single V-groove	backing	250 max.	160	22	1.2
	rest	250 max.	170	23	2.2

Table 2 — Parameters Used in AWS Test Specimens, with Different Heat Inputs (Refs. 16 and 17)

Electrode	E10018M			E11018M			E12018M			AWS Req.
Condition	Hot	Medium	Cold	Hot	Medium	Cold	Hot	Medium	Cold	
Heat input kJ/mm	2.1	1.7	1.3	2.2	2.0	1.6	2.1	1.6	1.2	
Current, A	185	160	140	180	160	140	180	160	130	
Voltage, V	25	24	22	25	24	23	23	23	22	
Preheat and interpass T °C(a)	107	101	93	107	101	93	107	101	93	93–107
Weld speed mm/s	2.2	2.3	2.4	2.0	1.9	2.0	2.0	2.3	2.4	
Number of layers	7	8	8	7	8	8	7	8	9	7–9

(a) Thermographical pencil traces that changed at the indicated temperatures were used. The measurements were carried out according to AWS Standard, Ref. 1.

Table 3 — All-Weld-Metal Chemical Composition from Electrodes Used for A, B and C

A — Variation of Mn (Ref. 13)

All Elements Expressed in wt-% Except N and O, which Are in ppm

Electrode Nominal Mn	P	S	C	Si	Cu	Ni	Cr	Mo	Mn	N	O
Mn 0.6	0.016	0.016	0.042	0.36	0.10	1.87	0.03	0.32	0.62	108	539
Mn 1.0	0.018	0.014	0.032	0.26	0.11	1.97	0.03	0.36	1.04	101	429
Mn 1.25	0.017	0.011	0.036	0.26	0.10	1.95	0.03	0.32	1.26	128	448
Mn 1.5	0.015	0.014	0.036	0.29	0.10	1.86	0.03	0.33	1.45	122	460
Mn 1.8	0.017	0.013	0.038	0.30	0.11	2.07	0.03	0.37	1.82	122	400
Mn 2.0	0.018	0.013	0.043	0.29	0.11	2.08	0.04	0.37	2.10	123	410

B — Variation of C (Ref. 14)

Nominal C	P	S	C	Si	Cu	Ni	Cr	Mo	Mn	V	N	O
0.05	0.024	0.013	0.95	0.25	0.06	1.84	0.05	0.34	1.21	0.01	143	444
0.07	0.025	0.013	0.07	0.26	0.06	1.90	0.05	0.34	1.24	0.01	119	365
0.10	0.023	0.009	0.10	0.34	0.05	1.92	0.05	0.35	1.42	0.01	87	345
0.12	0.031	0.011	0.12	0.33	0.05	1.88	0.05	0.34	1.41	0.01	99	329

C — Variation of Cr (Ref. 15)

Nominal Cr	P	S	C	Si	Cu	Ni	Cr	Mo	Mn	V	N	O
0	0.014	0.010	0.038	0.36	0.070	2.00	0.04	0.37	1.03	0.01	98	476
0.4	0.014	0.011	0.040	0.35	0.070	1.96	0.38	0.35	1.00	0.01	79	474
0.8	0.014	0.010	0.041	0.35	0.072	1.96	0.78	0.37	1.03	0.01	84	487
1.2	0.015	0.011	0.042	0.38	0.073	1.95	1.15	0.37	1.06	0.01	90	489
1.5	0.014	0.011	0.042	0.40	0.071	1.98	1.50	0.35	1.07	0.01	105	525
1.8	0.014	0.011	0.042	0.38	0.070	1.92	1.82	0.34	1.06	0.01	101	517
0	0.013	0.010	0.042	0.33	0.065	1.98	0.04	0.37	1.46	0.01	94	472
0.4	0.013	0.010	0.040	0.35	0.065	1.94	0.41	0.36	1.43	0.01	104	459
0.8	0.013	0.010	0.048	0.34	0.065	1.86	0.75	0.34	1.45	0.01	103	470
1.2	0.013	0.010	0.043	0.34	0.065	1.98	1.15	0.38	1.37	0.01	120	462
1.5	0.014	0.011	0.044	0.33	0.065	1.88	1.43	0.36	1.39	0.01	92	486
1.8	0.014	0.011	0.04	0.36	0.065	1.99	1.89	0.38	1.49	0.01	103	472

pressed in wt-%) and maintained the remaining chemical elements constant, were initially developed. Building on the results of this work, four experimental electrodes were designed and produced using the previously found optimum Mn level to produce weld deposits with carbon content of 0.05, 0.07, 0.10 and 0.12% respectively. The influence of Cr was investigated by means of 12 experimental electrodes designed to produce weld deposits with nominal Cr levels of 0, 0.4, 0.8, 1.2, 1.5 and 1.8% for Mn levels of 1% and 1.4% for each Cr content. Electrode diameter was 4 mm in all cases and the coating factor (diameter of the coating/diameter of the wire) was maintained at 1.65.

All-Weld-Metal Test Coupons

Two all-weld-metal samples were made with each electrode in the flat position according to ISO 2560-73. Although the objective was to develop AWS E100/110/12018M-type electrodes, ISO-type all-weld-metal samples with three passes per layer were preferred in order to obtain the highest possible columnar zone percentage in the Charpy V-notch location (Ref. 19). The welding parameters employed are shown in Table 1. One sample from each electrode was kept in the as-welded condition while the other was subjected to a stress relieving heat treatment for 1 h at 620°C (1150°F).

Mechanical Properties and Metallographic Studies

Two sub-size Minitrac (Ref. 20) tensile specimens (total length = 55 mm, gauge length = 25 mm, reduced section diameter = 5 mm, ratio of gauge length to diameter = 5:1) tested at room temperature, and enough Charpy V-notch specimens to build the Absorbed Energy vs. Test Temperature curve between –90°C (–130°F) and 20°C (68°F) were machined out of the ISO all-weld-metal samples. A cross section was also obtained from each specimen to conduct a hardness survey and the metallographic analysis. This was performed using light microscopy on the top bead, the grain-coarsened and grain-refined regions of the weld metal, and along a line coincident with the location of the notch of the Charpy samples (Ref. 21). In case of Cr variation, a study using the scanning electron microscope was also carried out at 1000 and 5000X.

To take into account any possible effect of dilution and/or dynamic strain aging at the root region on fracture toughness of the weld deposits (Ref. 22), production-type, single V-groove, multipass welds were made with each electrode on 19-mm-thick plate (typical chemical composition: C 0.1%; Mn 0.5%; Si 0.1%; P 0.01% and S 0.02%). Welding parameters used in this case are shown in Table 1. Welding was done in the flat position and the sequence was such that a backing run was deposited first and, after grinding to sound weld metal from the other side, the weld was completed. The test panels were prevented from moving during welding. Fracture toughness of the as-welded production-type, single V-groove joints was assessed by means of CTOD testing. For this purpose, full thickness, single-edge-notched, three-point-bend specimens were extracted from each weld, with the notch in the through-thickness direction. An initiating fatigue precrack, with initial crack depth to width ratio a/W = 0.5, was used in all cases. To promote plain strain conditions at the crack tip, 25% side grooving of the specimens was adopted. Testing was conducted at –10°C (14°F) according to BS 5762:79 (Ref. 23).

Variation of Heat Input

To study the influence of changes in heat input, all-weld-metal test coupons according to AWS A5.5-81 were prepared with E10018M, E11018M and E12018M commercial-type electrodes, designed according to the results ob-

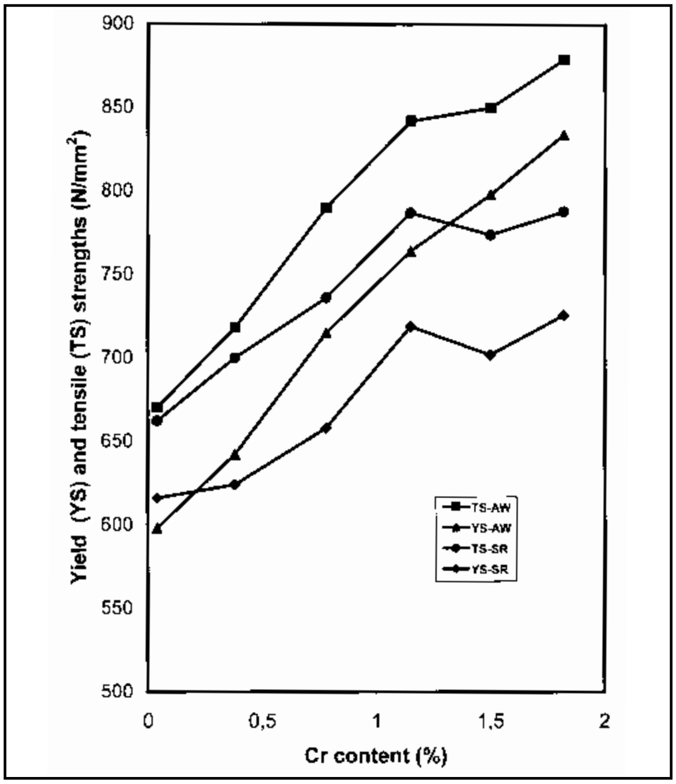

Fig. 3 — Tensile properties vs. all-weld-metal Cr content for 1% Mn, ISO test specimens (AW, as-welded; SR, stress relieved).

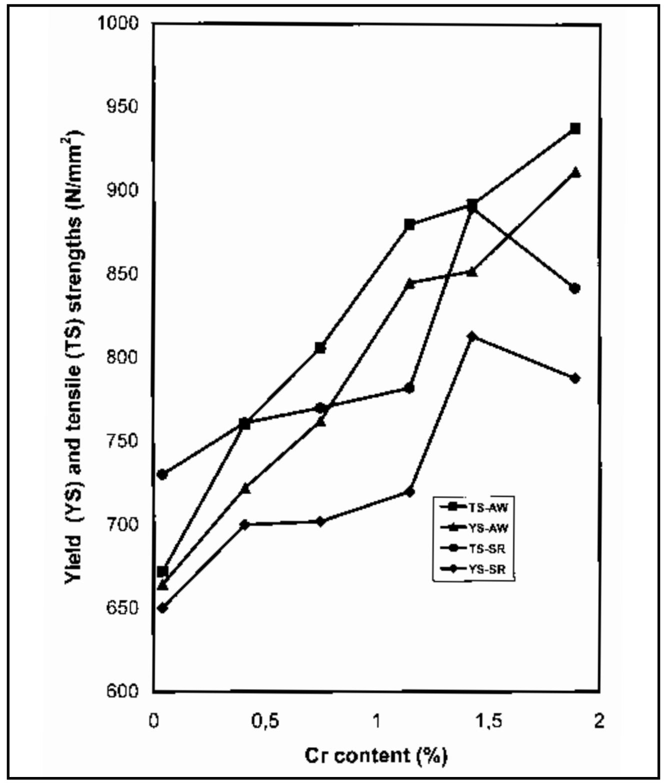

Fig. 4 — Tensile properties vs. all-weld-metal Cr content for 1.4% Mn, ISO test specimens (AW, as-welded; SR, stress relieved).

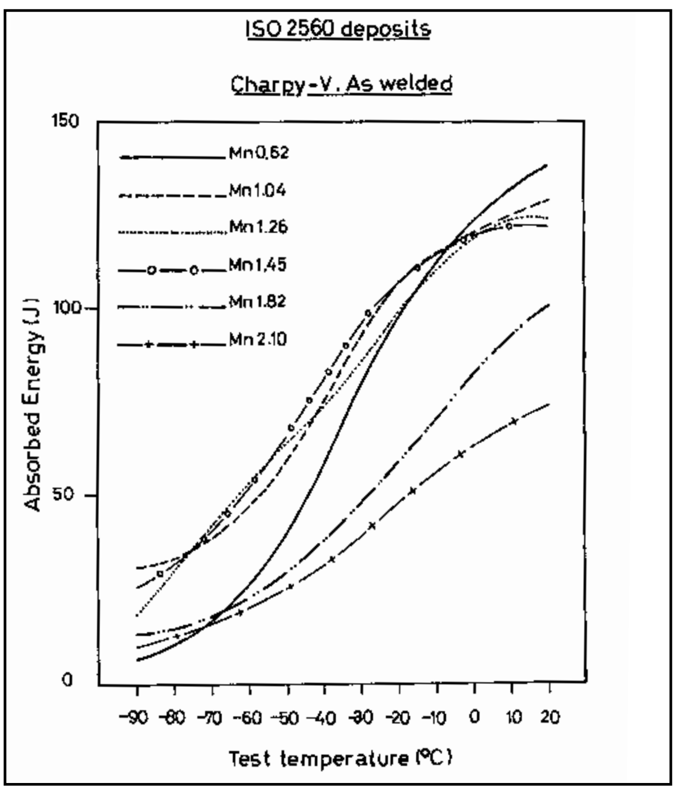

Fig. 5 — All-weld-metal Charpy V-notch impact test results for Mn variation (Ref. 13).

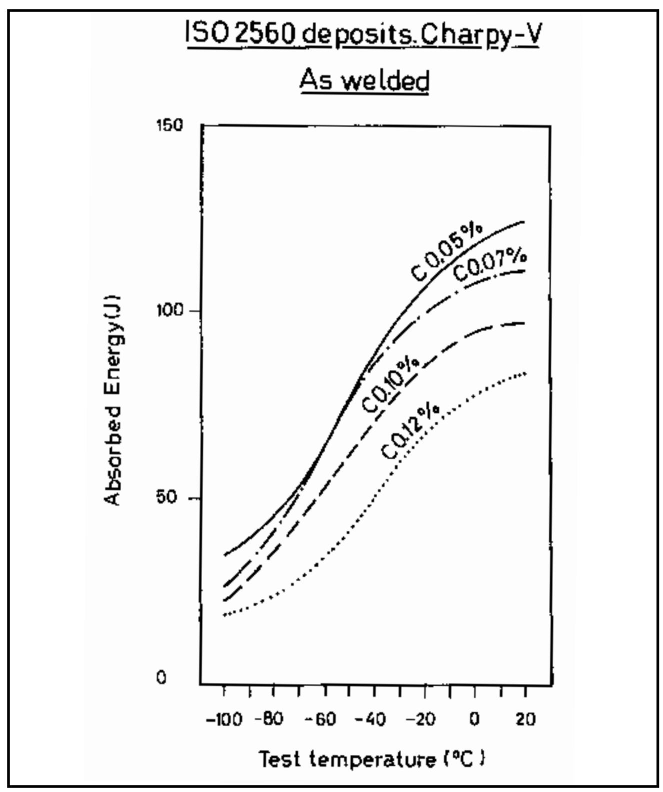

Fig. 6 — All-weld-metal Charpy V-notch impact test results for C variation (Ref. 14).

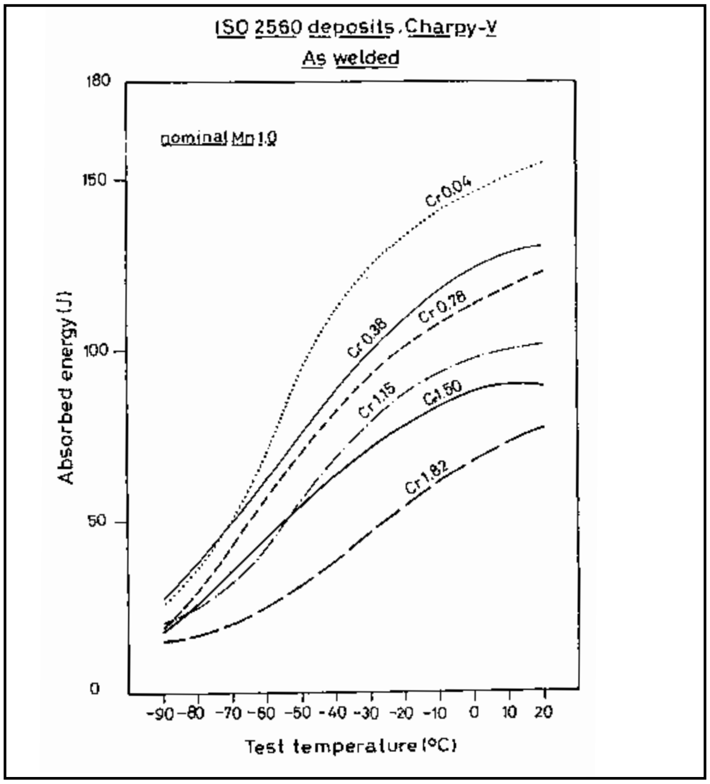

Fig. 7 — All-weld-metal Charpy V-notch impact test results for Cr variation, 1% Mn (Ref. 15).

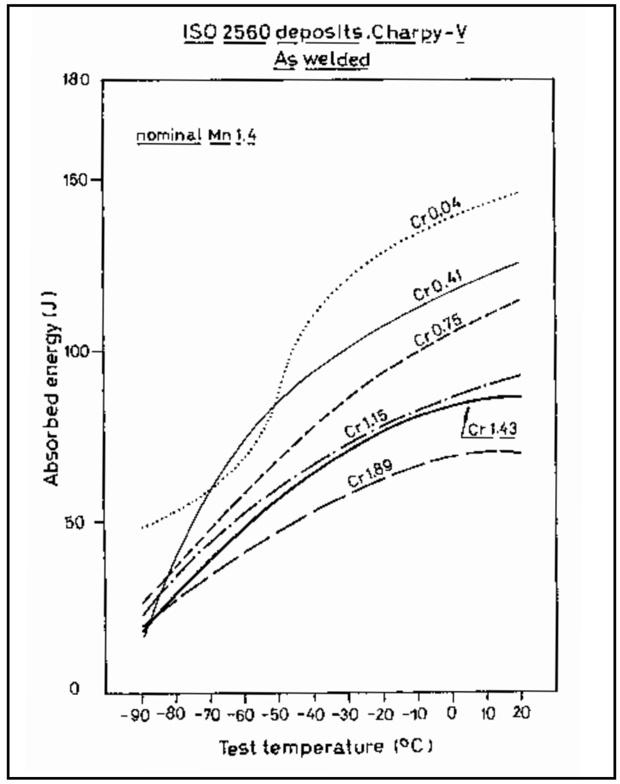

Fig. 8 — All-weld-metal Charpy V-notch impact test results for Cr variation, 1.4% Mn (Ref. 15).

tained as stated previously. The current range was selected to obtain good operative behavior in all cases, and the interpass temperature (maintained within the range allowed by the AWS standard, Ref. 1) (Table 2) and welding speed were varied in such a way as to obtain with each electrode three sets of samples: a "hot" weld (high heat input and interpass temperature), a "medium" weld (medium heat input and interpass temperature) and a "cold" weld (low heat input and interpass temperature). The welding parameters employed are shown in Table 2.

From each all-weld-metal test specimen, tensile specimens (with a 4:1 gauge length to diameter ratio and located as required by AWS A5.5-81), one section for both metallographic studies and a hardness survey, and five Charpy V-notch specimens were obtained. Tensile properties were measured at room temperature and Charpy V-notch tests were conducted at –51°C (–60°F).

Results and Discussion

Variation of Chemical Composition of Weld Metal at Constant Heat Input

Table 3 shows the all-weld-metal chemical composition for all the electrodes. Each one of the three groups of electrodes presents the variations in the elements previously mentioned while the other elements remained essentially constant. Minor inevitable variations in carbon and nickel for the Mn series were found to be within the measurement method error. Manganese variations in the C series, although higher, corresponded to the range in which no toughness differences were found in the Mn series (Ref. 13). It was observed that, as expected, increasing carbon and manganese led to a reduction in weld metal oxygen due to the double role played by these elements as deoxidants and alloying elements.

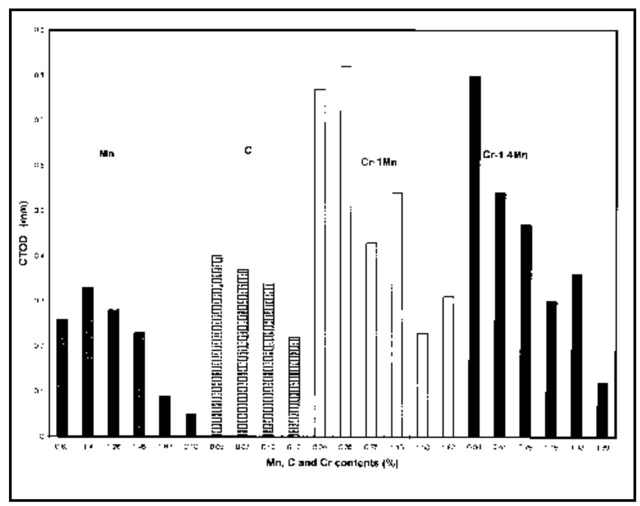

Fig. 9 — CTOD values for Mn, C and Cr contents in single V-groove butt joints (Refs. 13–15).

Figures 1–4 show the effects of manganese, carbon and chromium (for 1 and 1.4% Mn) on the all-weld-metal tensile test results in the as-welded and stress relieved conditions, respectively. It can be seen that an increase in the content of any of the elements considered led to a higher weld metal yield point and tensile strength. Stress relieving resulted in some reduction in the tensile properties. It would be thus rather easy to select the alloying values suitable to satisfy the minimum requirements for weld metal tensile strength and to locate the yield point within the range established by the AWS standard for the E10018M, E11018M and E12018M type electrodes. Charpy V-notch curves corresponding to the all-weld-metal ISO specimens in the as-welded condition are shown in Figs. 5–8 for each group of electrodes. It was observed that Mn in the range of 1 to 1.4%

Table 4 — Columnar Zone Microstructural Constituents of ISO All-Weld-Metal Test Specimens for C, Mn and Cr Variations

Element	All-Weld-Metal Content (wt-%)	Grain Boundary Ferrite (%)	Polygonal Ferrite (%)	Ferrite with Second Phase (%)	Acicular Ferrite (%)
Mn	0.62	72	2	7	19
	1.04	23	3	2	72
	1.26	14	2	2	82
	1.45	5	3	2	90
	1.82	2	9	3	86
	2.10	8	4	1	87
C	0.05	18	5	1	76
	0.07	10	3	2	85
	0.10	6	3	2	89
	0.12	2	2	3	93
Cr Mn 1 wt-%	0.04	28	4	3	65
	0.38	25	2	2	71
	0.78	21	2	2	75
	1.15	17	3	2	78
	1.50	14	4	2	80
	1.82	10	2	2	86
Cr Mn 1.4 wt-%	0.04	25	2	4	69
	0.41	18	3	3	76
	0.75	13	3	3	81
	1.15	10	2	3	85
	1.43	8	3	2	87
	1.89	6	2	3	89

Table 5 — Relative Size of the Columnar and Refined Regions Corresponding to the Location of the Notch in the Charpy-V Specimens and Primary Austenitic Grain Size in the Columnar Region of the All-Weld-Metal Top Bed (Ref. 15)

	Cr Content (wt-%)	Columnar Zone (%)	Refined Zone (%)	Average Columnar Grain Width (μm)
Mn 1 wt-%	0.04	34	66	115
	0.38	40	60	109
	0.78	45	55	104
	1.15	55	45	95
	1.50	56	44	92
	1.82	57	43	90
Mn 1.4 wt-%	0.04	37	63	102
	0.41	41	59	98
	0.75	47	53	93
	1.15	51	49	90
	1.43	57	43	88
	1.89	59	41	87

Table 6 — Hardness Ranges Measured in the Transversal Cuts Used for Metallographic Studies Extracted from the Mechanical Property Test Coupons

Mn (wt-%) Ref. 13	0.62	1.04	1.26	1.45	1.82	2.10
Hardness (HV 10)	192–220	206–227	228–266	240–280	265–310	274–322
C (wt-%) Ref. 14	0.05	0.07	0.10	0.12		
Hardness (HV 10)	222–253	247–298	272–325	288–331		
Cr (Mn 1 wt-%) Ref. 15	0.04	0.38	0.78	1.15	1.50	1.82
Hardness (HV 10)	212–257	224–258	238–267	258–295	271–300	302–333
Cr (Mn 1.4 wt-%) Ref. 15	0.04	0.41	0.75	1.15	1.43	1.89
Hardness (HV 10)	212-258	232–264	253–281	275–318	284–338	296–348

presented the optimum Charpy values. This was not the case for C and Cr that had a deleterious effect on toughness. Considering the minimum AWS standard requirement is 27 J at –51°C, these results show that to achieve the necessary all-weld-metal tensile strength coupled with the required toughness, a maximum of 1.5% Mn together with 0.10% C, 2.0% Ni and 0.35% Mo should be used. For C level under 0.05%, Cr additions up to 0.75% are also effective for the same Ni and Mo levels. It should be borne in mind that for these consumables, manufacturers' commercial brochures usually quote toughness values of about 50 J at –51°C (Refs. 24, 25). Stress relieving produced some deterioration on impact properties in the transition temperature range (Refs. 13–15). These results show that the shift in transition temperatures introduced by the heat treatment increases markedly with the Mn content beyond 1.5%. Increasing carbon content produced a shift toward higher transition temperatures and a reduction in the upper shelf energy. Within the carbon content range considered in this study, best impact properties were obtained with 0.05% C in the weld deposit. In general, a monotonous reduction in toughness with increasing Cr was also found both in as-welded and in the stress-relieved conditions, as measured by the Charpy V-notch impact test results. Increasing the Mn content from 1% to 1.4% produced a further, albeit minor, deterioration in toughness.

CTOD tests results are shown in Fig. 9. It is worth noting that, with the exception of the CTOD specimens corresponding to a nominal manganese content of 1.8% and 2.0%, which fractured in δ_c mode, all the samples fractured in either δ_u or δ_m modes, δ_c designating the CTOD values corresponding to cleavage fracture of the specimen without prior stable crack growth, δ_u those corresponding to cleavage fracture with prior crack extension, and δ_m those corresponding to the first attainment of a maximum load plateau. Increasing Mn, C and Cr produced a reduction in CTOD values, but these values remain adequate within the range of composition suggested above to prevent toughness deterioration.

With the results so far presented, it is possible to select the optimum chemical composition of the weld metal for each type of electrode E10018M, E11018M and E12018M. It will suffice to enter the corresponding curves and look for the composition ranges in Mn, C and Cr that guarantee the achievement of tensile and impact properties according to the requirements of the relevant AWS standard.

Table 4 shows the results of the quantitative assessment carried out according

to the recommendations of IIW Doc. IX-1533-88 (Ref. 21), on the top bead of the ISO specimens in the as-welded condition at magnifications of 400 and 500X for each one of the tested samples.

Manganese additions up to about 1.5% promoted the formation of acicular ferrite and reduced the amount of grain boundary ferrite as previously found (Ref. 9). Beyond this level, there seemed to be some further reduction in the relative amount of grain boundary ferrite but also an increase in polygonal ferrite and ferrite with aligned M-A-C. This is in agreement with the notch toughness test results that showed impact properties deteriorated when the Mn level increases beyond 1.5%. Manganese also produced a generalized grain size decrease as can be seen in Fig. 10.

Increasing carbon led to a higher proportion of acicular ferrite and to a reduction in grain boundary ferrite. For a carbon content of about 0.12%, a microstructure consisting of practically 100% acicular ferrite was obtained. Some small proportion of polygonal ferrite and ferrite with aligned M-A-C was also present, but the amount of these constituents did not seem to be significantly affected by variations in the carbon level. These results are in agreement with previous findings by Evans (Ref. 12) in C-Mn weld metal. In the weld metal analyzed in this work, the presence of Ni and Mo contributed further to the reduction in the proportion of grain boundary ferrite with a corresponding increase in acicular ferrite, according to what was shown by other authors (Refs. 26–28). Although increasing C levels effectively promoted acicular ferrite formation, it

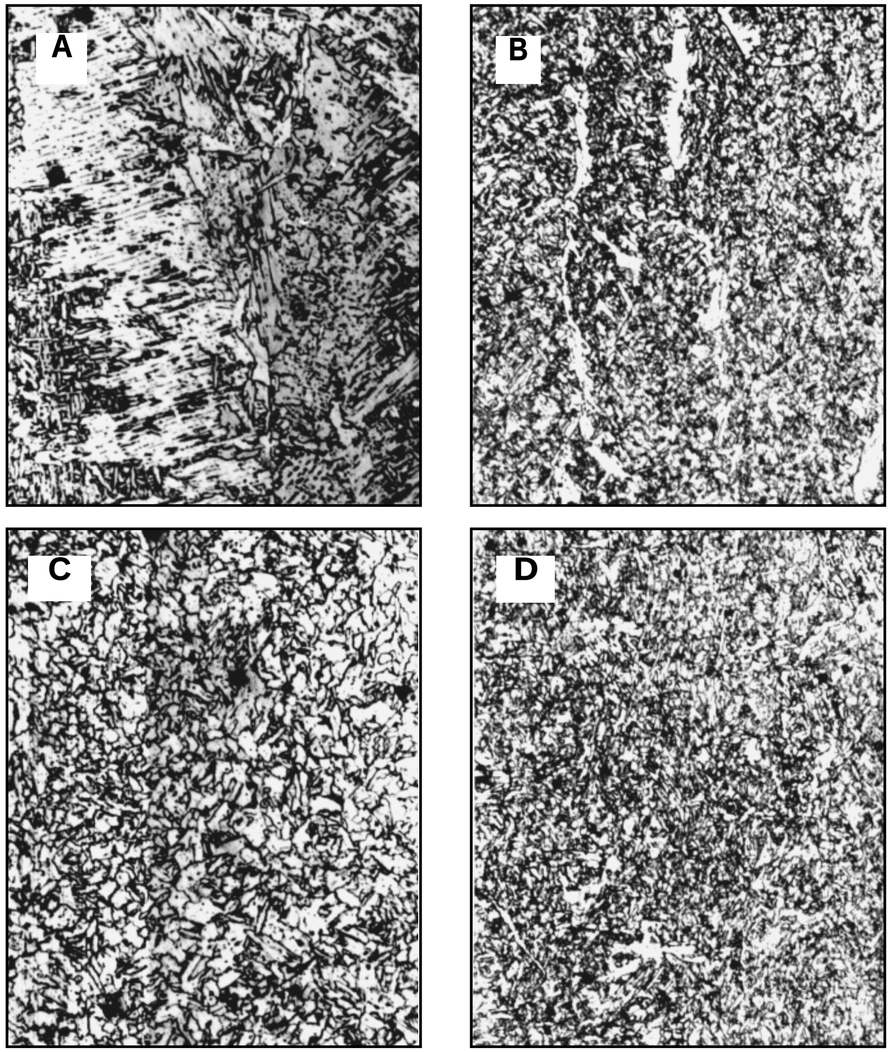

Fig. 10 — All-weld-metal typical microstructures for Mn variation series, as welded, 500X (Ref. 13). A — Columnar zone, 0.62% Mn; B — columnar zone, 1.82% Mn; C — reheated zone, 0.62% Mn; D — reheated zone, 1.82% Mn.

Table 7 — All-Weld-Metal Chemical Composition from Commercial Electrodes Used in AWS Test Specimens with Different Heat Inputs (Refs. 16 and 17)

	All Elements Expressed in wt-% Except N and O in ppm								
Electrode	C	Mn	P	S	Si	Ni	Cr	Mo	O	N
E10018M hot	0.042	1.34	0.025	0.013	0.34	1.90	0.08	0.38	552	129
E10018M medium	0.041	1.45	0.028	0.013	0.40	1.97	0.08	0.40	538	120
E10018M cold	0.056	1.49	0.029	0.013	0.40	1.97	0.09	0.40	511	87
E11018M hot	0.040	1.58	0.015	0.007	0.44	1.94	0.30	0.33	360	86
E11018M medium	0.042	1.63	0.016	0.007	0.48	1.97	0.31	0.35	321	84
E11018M cold	0.045	1.68	0.016	0.008	0.54	1.98	0.31	0.34	315	71
E12018M hot	0.043	1.56	0.022	0.016	0.43	2.25	0.45	0.43	377	98
E12018M medium	0.048	1.62	0.018	0.013	0.45	2.20	0.43	0.42	349	95
E12018M cold	0.051	1.68	0.020	0.012	0.46	2.13	0.46	0.40	314	87

Note: In all cases, Sn As, Sb, Co, Nb, Ti and Al were lower than 0.01 wt-%.

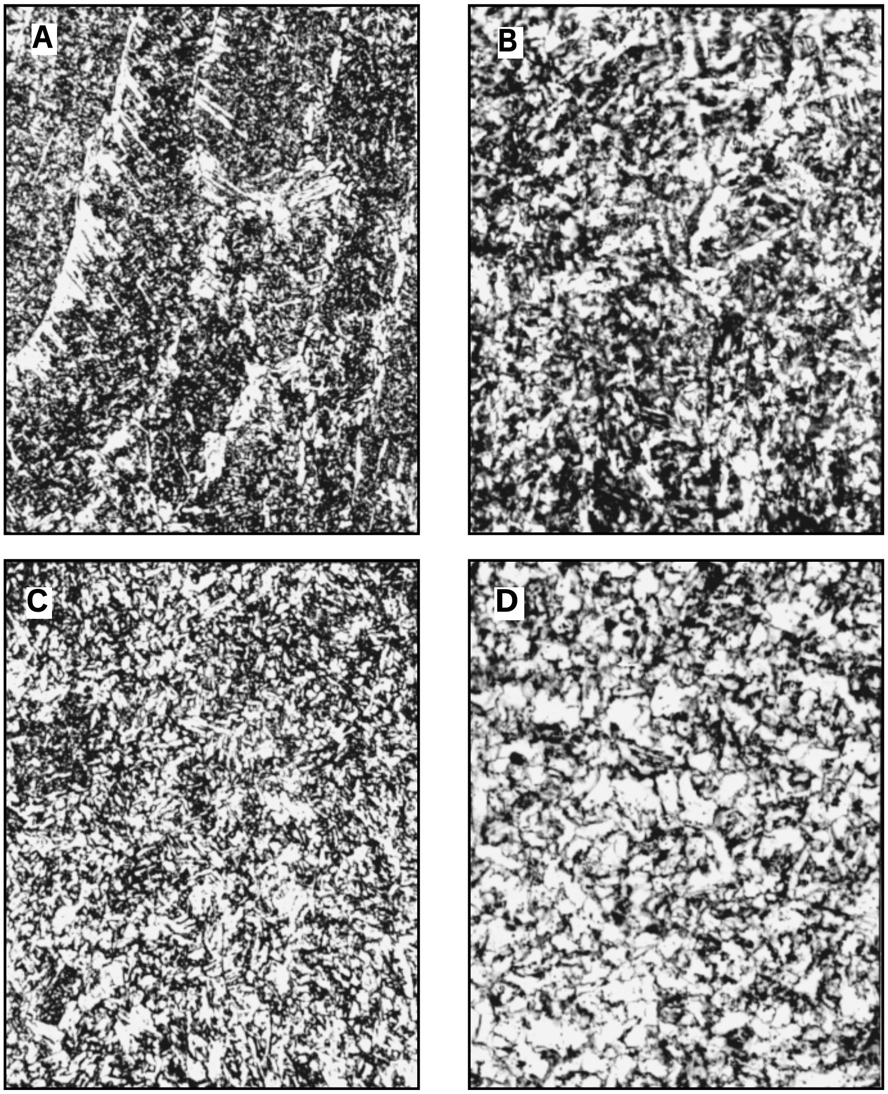

Fig. 11 — All-weld-metal typical microstructures for C variation, as welded, 500X (Ref. 14). A — Columnar zone, 0.05% C; B — columnar zone, 0.12% C; C — reheated zone, 0.05% C; D — reheated zone, 0.12% C.

Table 8 — All-Weld-Metal Mechanical Properties from Electrodes E10018M, E11018M and E12018M Obtained from Test Specimens Welded with Different Heat Inputs (Ref. 16 and 17)

Electrode	Heat Input (kJ/mm)	Condition	TS (N/mm²)	YS (N/mm²)	E (%)	Ch-V –51 °C (J)	Average Hardness (HV 10)
	2.1	hot	724	632	23.4	53	234
E10018M	1.7	medium	760	660	22.8	56	246
	1.3	cold	766	665	22.0	73	251
AWS req.			690 min.	610–690	20 min.	27 min.	
	2.2	hot	734	669	23.1	55	255
E11018M	2.0	medium	764	715	23.6	60	264
	1.6	cold	810	770	21.6	45	275
AWS req.			760 min.	680–760	20 min.	27 min.	
	2.1	hot	796	754	20.7	55	281
E12018M	1.6	medium	845	814	19.7	50	289
	1.2	cold	895	866	19.0	54	297
AWS req.			830 min.	745–830	18 min.	27 min.	

TS: tensile strength; YS: yield strength; E: elongation; Ch-V: impact Charpy V-notch

also resulted in acicular ferrite coarsening, as shown in Fig. 11. This coarsening effect was particularly apparent in the grain-refined zone — Fig. 11. This finding is at first glance contradictory with the observations of Evans and Taylor (Refs. 12, 29) who established that for C-Mn weld deposits an increase in the C content resulted in a reduction of primary grain size and a refinement in the recrystallized zones.

It was observed using light microscopy that increasing Cr led to an apparent higher proportion of acicular ferrite and to a reduction in grain boundary ferrite in the columnar zone — Table 4. Nevertheless, the microstructural analysis of high-strength weld metal by light microscopy has been proved to be inefficient (Refs. 30, 31) since the necessary resolution to clearly define the microconstituents of low-temperature transformation is not available. When this system was analyzed through the Cr variations for 1.4% Mn, under the scanning electron microscope with magnifications of 1000 and 5000X (Ref. 16), it was observed that Cr promoted the formation of ferrite with second phases at the expense of acicular ferrite and primary ferrite, these two microconstituents being completely absent for Cr levels of 0.75%. From this level of Cr upward, martensite was present and became the dominant microconstituent at Cr levels of 1.43% and more (Ref. 16) (Fig. 12), as previously found (Refs. 32, 33). This change in the microstructure explained the drop in toughness with the increase in weld metal Cr, since ferrite with second phases and martensite are recognized as deleterious for toughness (Refs. 5, 6). Table 5 shows the increase in the proportion of columnar zone promoted by higher Cr contents (coincidently with Ref. 33), which also contributed to the deterioration in toughness. This effect is composed with the strengthening action of Mn, C and Cr, as shown by the hardness measurement results shown in Table 6. Table 5 also shows the reduction in primary austenitic grain size of the columnar zone signaling Cr as a grain size refiner.

Variation of Heat Input

Table 7 shows the all-weld-metal chemical composition from test specimens of commercial-type electrodes, welded with three different heat inputs, that were within the range found as optimum in the study of the influence of the variation of the chemical composition. The oxygen and nitrogen values increased with the heat input. The higher current and voltage might result in more

O and N in the arc environment (Refs. 34, 35) as more time was available for the weld pool to absorb them from the environment (Ref. 35). It is interesting to note that due to a different coating factor, mineral base and Mn content of the coating of the E10018M, E11018M and E12018M commercial electrodes used, two different levels of oxygen were achieved (511–552 ppm and 314–377 ppm). Nevertheless, the three electrodes were iron powder basic coating electrodes according to EXXX18-X classification (Ref. 1 and/or 2). It was possible to observe in the three cases that as the heat input increased and consequently the pool oxygen content rose, the values of C, Mn and Si decreased, due to the increased oxidation of these three elements. This effect was previously found by Evans (Refs. 36, 37). The "medium" test specimens presented intermediate Mn and Si levels.

Table 8 presents the mechanical properties obtained with the three AWS test coupons prepared with different heat inputs. It can be seen that the variation of heat input produced changes in the all-weld-metal mechanical properties as expected, due to the fact that they are dependent on the chemical composition and microstructure. Therefore, the rate at which welds cool and transform from austenite following solidification exerts a strong influence on their properties. In turn, cooling rate is dependent upon the conditions of welding (Refs. 38–45).

In agreement with what was found in high-strength steel weld metal obtained with the GMA (Refs. 38, 39) and SAW processes (Refs. 40, 42), yield and tensile strengths decreased, as well as average hardness values as measured along the cross section centerline, when heat input increased (Table 8). As expected, average hardness values rose from E10018M to E11018M to E12018M all-weld-metal electrodes, due to alloy content increase.

All the test samples produced with the E10018M electrode satisfied the yield and tensile strength requirements of the standard, while those samples produced with E11018M and E12018M electrodes exhibited a different behavior: Only the "medium" sample satisfied the requirements of the relevant AWS standard for these electrodes. With the E11018M and E12018M "cold" samples, the maximum yield point limits were exceeded. With the "hot" samples, the required minimum tensile strengths were not achieved, and with the E11018M "hot" sample, the minimum required yield strength value was not reached. Elongation and toughness requirements were easily satisfied with all the electrodes and all the heat inputs (Table 8).

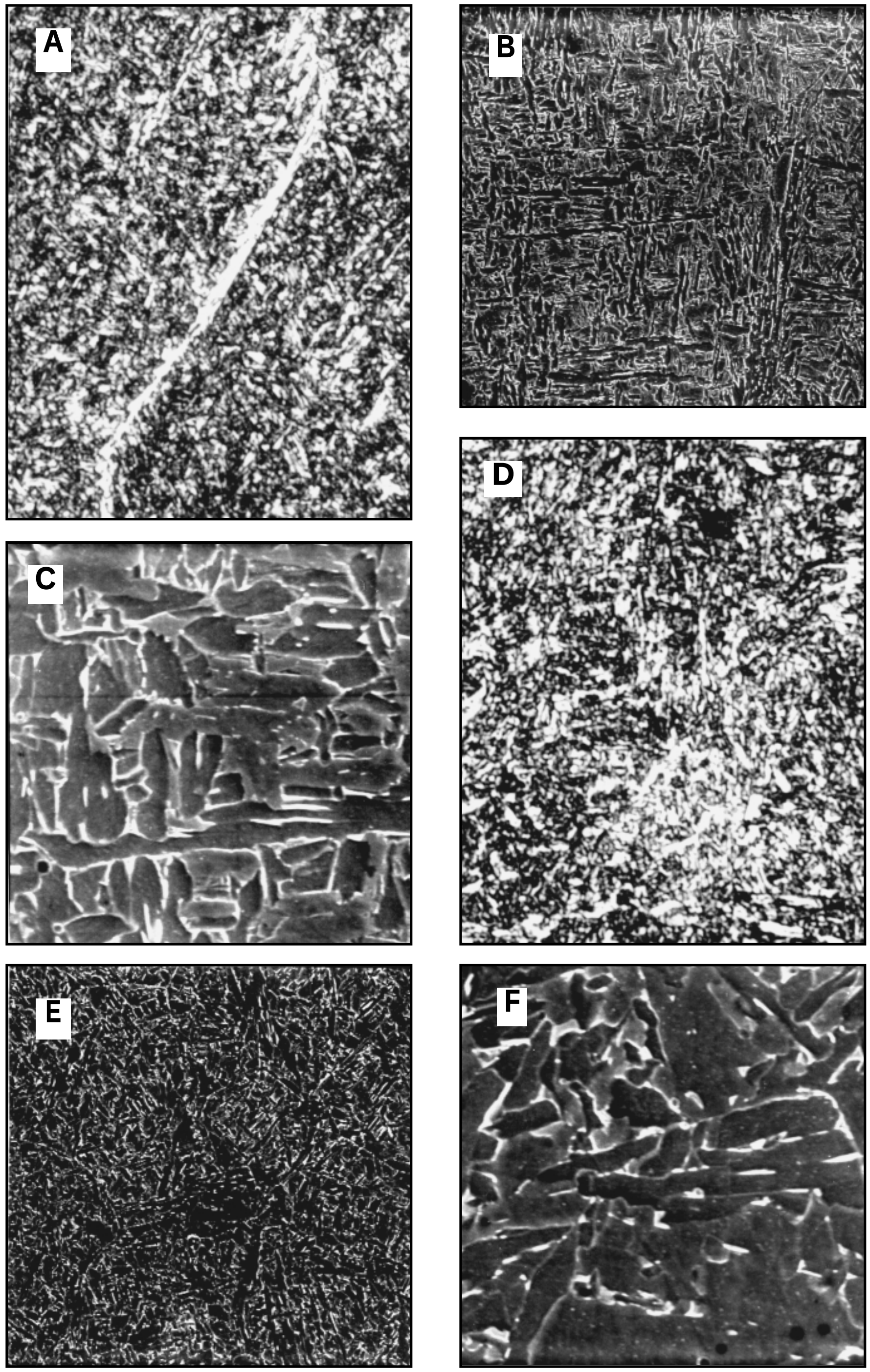

Fig. 12 — All-weld-metal typical microstructures for 0.75%, Cr 1.4% Mn, as welded (Refs. 15, 16). A — Columnar zone, 500X; B — columnar zone 1000X; C — columnar zone 5000X; D — reheated zone, 500X; E — reheated zone, 1000X; F — reheated zone, 5000X.

Table 9 — Percentages of Variations of Yield Strength (YS) with Respect to the Medium Value of the YS Range Required by AWS Standard for the Three Electrodes (Ref. 16)

Electrode	AWS YS Required Range (N/mm^2)	YS Required Range Medium Value (N/mm^2)	YS Range (N/mm^2)	% YS (from Medium Value)
E10018M	610–690	650	80	±− 6.2
E11018M	680–760	720	80	±− 5.6
E12018M	745–830	787.5	85	±− 5.4

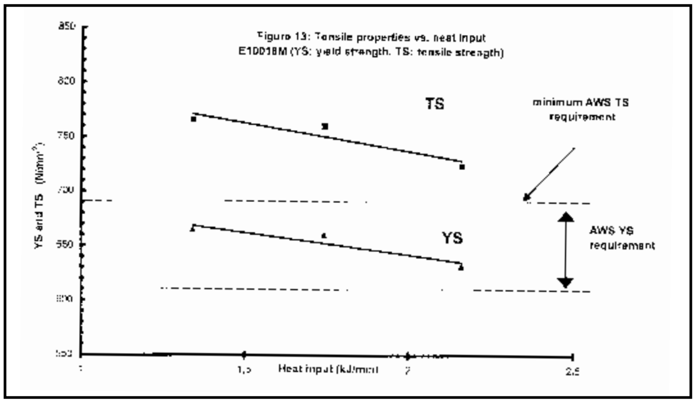

Fig. 13 — Tensile properties vs. heat input E10018M (YS, yield strength; TS, tensile strength).

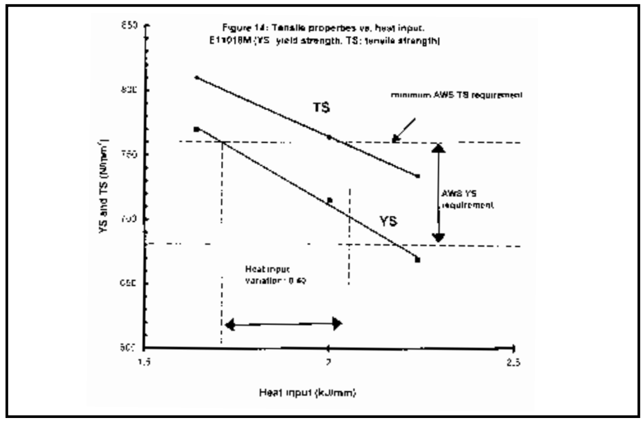

Fig. 14 — Tensile properties vs. heat input E11018M (YS, yield strength; TS, tensile strength).

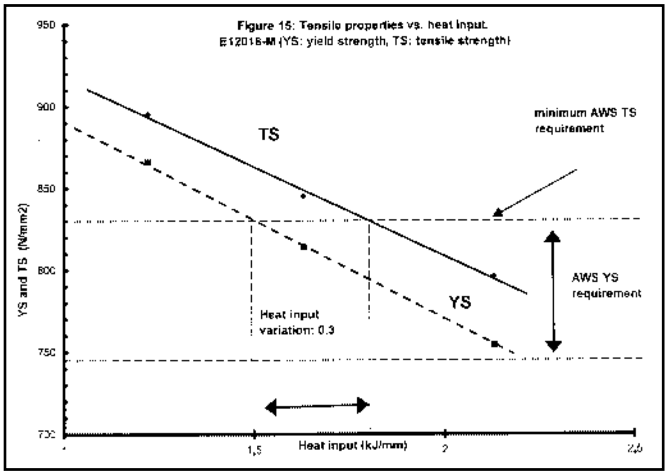

Fig. 15 — Tensile properties vs. heat input E12018M (YS, yield strength; TS, tensile strength).

It follows that with the electrode E10018M, the full range of heat inputs used in this work may be employed without risk of impairing the properties of the weld metal beyond the allowable limits. On the other hand, with electrodes E11018M and E12018M, care must be exerted to control the cooling rate during welding, and precise instructions should be issued to establish suitable welding parameters within a narrower range than that used in this work to guarantee meeting the requirements. According to Table 8, when going from electrode E10018M to the E12018M, that is with increasing alloy content, all-weld-metal tensile properties became more sensitive to variations in heat input with a reduction in the heat input usable range, as shown in Figs. 13–15. Actually, to satisfy the AWS tensile property requirements becomes more difficult as weld alloy content increases, due to two facts: the already referred increased weld metal sensitivity and the increasing AWS tensile requirements. Table 9 shows the relative variation of yield strength with respect to the mean value of the yield strength range required by AWS standard for the three electrodes. It can be observed that as the yield strength increases the percentage variation decreases, thus rendering the standard more demanding. (It should be stressed that the previous considerations apply to the specific test conditions under which the samples were produced ([20-mm-thick plate and 93° to 107°C preheat and interpass temperature]).

The metallographic study (Table 10) showed a decrease in the proportion of the columnar zones (and consequently an increase of the reheated ones) and an increase in the ferrite grain size as the heat input increased, as previously found (Refs. 36, 37, 40, 42). It was not possible to carry out this last measurement for E12018M all-weld-metal because the veins of grain boundary ferrite disappeared as the degree of alloy increased (Refs. 27, 32, 33, 46). A small increase in both acicular ferrite and ferrite with second phase, at the expense of the primary ferrite in the columnar zone, was also observed with the light microscope at 400X. With higher magnifications, other constituents could be identified and quantified (Refs. 16, 27, 33).

Table 10 — Results of Metallographic Studies (Refs. 16 and 17)

Electrode	Heat Input (kJ/mm)	Columnar Zone (%)	Refined Zone (%)	Prior Austenite Grain Width (μ)(a)	Acicular Ferrite (%)(b)	Ferrite with Second Phase (%)(b)	Primary Ferrite (%)(b)
	2.1 hot	25	75	140	62	20	18
E10018M	1.7 medium	42	58	125	58	16	26
	1.3 cold	55	45	110	56	14	30
	2.2 hot	18	82	216	74	20	6
E11018M	2.0 medium	25	75	189	72	19	9
	1.6 cold	42	58	159	66	17	17
	2.1 hot	36	64		64	26	10
E12018M	1.6 medium	45	55	(c)	62	25	13
	1.2 cold	50	50		59	22	19

(a) Measured in the columnar zone. (b) Microconstituents in columnar zone. (c) For E12018M electrode, it was not possible to perform this measurement due to the loss of the grain boundary ferrite veins.

Conclusions

The influences of chemical composition at constant heat input were as follows:

- An increase in Mn, C or Cr individually produced an increase of tensile and yield strengths and hardness.
- In the absence of Cr and at the lowest value of C, maximum toughness was obtained for Mn contents between 1.0 and 1.5%. Toughness fell as C increased. Up to 0.10% C the obtained values satisfied the AWS requirements, when Mn

was in the optimum range and without addition of Cr. In general, Cr was detrimental to toughness in this system, but good impact properties were obtained with Cr up to 1.0% for both Mn contents studied. In all cases stress relief treatment produced a decrease in tensile properties and Charpy V-notch toughness results. While an increase in these three elements produced a drop in CTOD results, it was possible to maintain satisfactory values for all C levels, and up to about 1.4% Mn and Cr, respectively.

• Manganese and carbon promoted the formation of acicular ferrite, as shown by examination at low magnification with the light microscope. It was observed that increasing Cr led to an apparent higher proportion of acicular ferrite and to a reduction in grain boundary ferrite in the columnar zone. At high enough resolution it was detected that Cr promoted the formation of ferrite with second phases at the expense of acicular ferrite and primary ferrite, these two microconstituents being completely absent for Cr levels of 0.75%. From this level of Cr upward, martensite was present .

• Manganese and chromium acted as grain refiners. The addition of C produced a general grain size coarsening.

The influences of varying heat input were as follows:

• AWS E10018M-type electrodes were found suitable to produce all-weld-metal test coupons over a wide range of welding parameters while still meeting the AWS mechanical property requirements. However, welding parameters for AWS E11018M and E12018M electrodes had to be precisely specified and closely controlled if all-weld-metal test coupons were to reproducibly satisfy AWS requirements.

These results involve a rational methodology for welding consumable development that is based on the influence that controlled changes in chemical composition and heat input have on weld metal mechanical properties and microstructure of E10018/11018/12018M deposits.

The study on the influence of heat input variation was performed according to AWS A5.5-81 requirements. Chemical composition and mechanical property requirements of the two versions of A5.5 standard are the same, but the design of the Groove Weld Test Assembly for Mechanical Properties and Soundness of Weld Metal is slightly different. This difference may account for differences in tensile property results. It is the opinion of the authors of this paper that the all-weld-metal behavior general tendency will be the same if the new design is used to evaluate the variation of tensile properties with heat input, but this cannot be assured without the performance of adequate tests.

Acknowledgments

The authors want to give proper recognition to the Fundación Latinoamericana de Soldadura, the INTEMA of Facultad de Ingeniería de la Universidad Nacional de Mar del Plata, and Conarco Alambres y Soldaduras S.A. from Argentina and to the Pontifícia Universidade Católica do Rio and Centro Federal de Educação Tecnológica from Brazil. All are organizations that have supported the different stages of this working program, from 1987 to 1996.

References

1. AWS A5.5-81, *Specification for Low Alloy Steel Covered Arc Welding Electrodes*. American Welding Society, Miami, Fla.

2. ANSI/AWS A5.5-96, *Specification for Low-Alloy Steel Electrodes for Shielded Metal Arc Welding*. American Welding Society, Miami, Fla.

3. George, M., Still, J., and Terry, P. 1981. Gas metal arc welds for high toughness applications — microstructure and other factors. *Metal Construction* 13(12): 730–737.

4. Keeler, T. 1981. Innershield welding. Part 1 — development and applications. 1981. *Metal Construction* 13(11): 667–673.

5. Garland, J. C., and Kirkwood, P. R. 1975. Towards improved submerged arc weld metal — part 1. *Metal Construction* 7(5): 275–283.

6. Garland, J. C., and Kirkwood, P. R. 1975. Towards improved submerged arc weld metal — part 2. *Metal Construction* 7(5): 320–330.

7. Pickering, F. B. 1978. *Physical Metallurgy and the Design of Steels.* Materials Science Series, Applied Science Publishers, London, U.K.

8. Abe, N., Kitada, T., and Miyata, S. 1980. Effects of alloying elements on the toughness and microstructure of high current density gas shielded arc process weld metals. *Transact. of the JWS* 11(4): 29–34.

9. Evans, G. 1980. Effect of manganese on the microstructure and properties of all-weld-metal deposits. *Welding Journal* 59(3): 67-s to 75-s.

10. Surian, E., and Boniszweski, T. 1992. Effect of manganese and type of current on the properties and microstructure of all-weld-metal deposited with E7016-1 electrodes. *Welding Journal* 71(9): 348-s.

11. Den Ouden, G., Verhagen, J. G., and Tichelgar, G. W. 1975. Influence of chemical composition on mild steel weld metal notch toughness.*Welding Journal* 54 (3):87-s to 94-s.

12. Evans, G. 1981. The effect of carbon on the microstructure and properties of C-Mn all-weld-metal deposits. IIW-IIS Doc. II-A-546-81.

13. Surian, E., Trotti, J., Cassanelli, A. Ni, and de Vedia, L. 1987. Influence of Mn content on mechanical properties and microstructure of a high strength SMA electrode weld metal. IIW-IIS Doc. II-A-724-87.

14. Surian, E., Trotti, J., Herrera, R. y de, Vedia, L. A. 1991. Influence of C on mechanical properties and microstructure of weld metal from a high-strength SMA electrode. *Welding Journal* 70(6): 133-s to 140-s.

15. Surian, E., Trotti, J., Cassanelli, L. A., and de Vedia, L. A. 1994. Influence of chromium on mechanical properties and microstructure of weld metal from a high strength SMA electrode. *Welding Journal* 73(3): 45-s to 53-s.

16. Bott, I. de S., Souza, L., Jorge, J., and Surian, E. Microstructural evaluation of a high strength weld metal with varying Cr content by means of scanning electron microscopy. IIW-IIS Doc. II-A-936–94.

17. Vercesi, J., and Surian, E. 1996. The effect of welding parameters on high-strength SMAW all-weld-metal — part 1: AWS E11018M. *Welding Journal* 75 (6): 191-s to 196-s.

18. Vercesi, J., and Surian, E. 1997. The effect of welding parameters on high-strength SMAW all-weld-metal — part 2: AWS E10018M and E12018M. *Welding Journal* 77(4): 164-s to 171-s.

19. Evans, G. M. 1978. Comparison of ISO 2560 and AWS A5.1-69. *Oerlikon-Schweissmitt* 3(85): 4–10.

20. Schnadt, H. M., and Leinhard, E.W. 1963. Experimental investigation of the sharp-notch behavior of 60 steels at different temperature and strain rates. IIW-IIS Doc. 196-343-63.

21. Abson, D. J. Guide to the light microscope examination of ferrite steel weld metals. IIW Doc. IX-1533-88.

22. Vega, R. A., Otegui, J. L., and de Vedia, L. A. Influence of dynamic strain ageing on notch toughness of weld deposits. *Latinamerican J. of Metallurgy and Materials* 1(3): 42–47.

23. British Standard Institution. *Methods for Crack Tip Opening Displacement (COD) Testing*, BS 5762:79, London, England.

24. Welding Electrodes. Catalog of Philips Lastechniek B. V. Holland.

25. Welding Consumables. Catalog of Kobe Steel. Kobelco. Japan.

26. Evans, G. M. 1990. The effect of nickel on the microstructure and properties of C-Mn all-weld metal deposits. *Oerlikon-Schweißmitteilungen* 45(115) 18–35.

27. Evans, G. M. 1988. The influence of molybdenum on the microstructure and properties of C-Mn all-weld-metal deposits. *Join. Mat.* 1(5): 239-s to 246-s.

28. Judson, P., and McKoewn, D. 1982. Advances in the control of weld metal toughness. *Second International Conference on Offshore Welded Structures.* The Welding Institute, London, England.

29. Taylor, D. S., and Evans, G. M. 1982. The systematic development of a new range of MMA electrodes for critical areas for offshore fabrication. *Second International Conference on Offshore Welded Structures.* The Welding Institute, London, England.

30. Jorge, J. C. F., and Rebello, J. M. A. 1989. Microscopia eletrônica de varredura de cordões de solda de alta resistência. *Soldagem e Materiais* 1(3): 44–49.

31. Jorge, J. C. F. 1993. Relacão tenacidade/microstrutura de metal de solda de aço C-Mn-Cr obtidos de solda passe único pelo proceso arco submerso. *Tese D. Sc. COPPE/UFRJ*. Brazil.

32. Jorge, J. C. J., Rebello, J. M. A., and Evans, G. M. 1993. Microstructure and tough-

ness relationship in C-Mn-Cr all-weld metal deposits. IIW / IIS Doc. II-A-880-93.

33. Jorge, J. C. J., Souza, L. F. G., Rebello, J. M. A., and Evans, G. M. 1994. Effect of Chromium on the Microstructure/ Toughness Relationship in C-Mn-Mo Weld Deposits. IIW / IIS Doc. II-A-930-94.

34. van Nassau, L., and van der Mee, V. 1991/1992. Nitrogen in manual metal arc welding. WRC Bulletin, N 369.

35. Boniszewski, T. *Self-Shielded Arc Welding.* p. 31, Abington Publishing, Cambridge, England.

36. Evans, G. M. 1982. The effect of heat input on the microstructure and properties of C-Mn all-weld-metal deposits. *Welding Journal* 61(4): 125-s to 132-s.

37. Evans, G. M. 1982. Effect of electrode diameter on the microstructure and properties of C-Mn all-weld-metal deposits. *Welding Review* 1(2): 4–8.

38. Stout, R. D., McLaughlin, P. F., and Strunck, S. S. 1969. Heat treatment effects on multipass welds. *Welding Journal* 48(4): 155-s to 160-s.

39. Lyttle, J. E., Dorschu, K. E., and Fragetta, W. A. 1969. Some metallurgical characteristics of tough, high-strength welds. *Welding Journal* 48 (11): 493-s to 498-s.

40. Smith, N. J., McGrath, J. T., Gianetto, J. A., and Orr, R. F. 1989. Microstructure/mechanical property relationships of submerged arc welds in HSLA 80 steel. *Welding Journal* 68(3): 112-s to 120-s.

41. Oldland, P. T., Ramsay, C. W., Matlock , D. K., and Olson, D. L. 1989. Significant features of high-strength steel weld metal microstructures. *Welding Journal* 68(4): 158-s to 168-s.

42. Gianetto, J. A., Smith, N. J., McGrath, J. T., and Bowker, J. T. 1992. Effect of composition and energy input on structure and properties of high-strength weld metals. *Welding Journal* 71(11): 407-s to 419-s.

43. Strunck, S. S., and Stout, R. D. 1972. Heat treatment effects in multipass weldments of a high-strength steel. *Welding Journal* 51 (10): 508-s to 520-s.

44. Glover, A. G., McGrath, J. T., Tinkler, M. J., and Weatherly, G. C. 1977. The influence of cooling rate and composition on weld metal microstructures in a C/Mn and a HSLA steel. *Welding Journal* 56(9): 267-s to 273-s.

45. Dorschu, K. E. 1968. Control of cooling rates in steel weld metal. *Welding Journal* 47(2): 49-s to 62-s.

46. Evans, G. M. 1989. The effect of chromium on the microstructure and properties of C-Mn all-weld-metal deposits. *Weld. Met. Fab.* 57(7): 346–358.

Preparation of Manuscripts for Submission to the *Welding Journal* Research Supplement

All authors should address themselves to the following questions when writing papers for submission to the Welding Research Supplement:

- Why was the work done?
- What was done?
- What was found?
- What is the significance of your results?
- What are your most important conclusions?

With those questions in mind, most authors can logically organize their material along the following lines, using suitable headings and subheadings to divide the paper.

1) **Abstract.** A concise summary of the major elements of the presentation, not exceeding 200 words, to help the reader decide if the information is for him or her.

2) **Introduction.** A short statement giving relevant background, purpose and scope to help orient the reader. Do not duplicate the abstract.

3) **Experimental Procedure, Materials, Equipment.**

4) **Results, Discussion.** The facts or data obtained and their evaluation.

5) **Conclusion.** An evaluation and interpretation of your results. Most often, this is what the readers remember.

6) **Acknowledgment, References and Appendix.**

Keep in mind that proper use of terms, abbreviations and symbols are important considerations in processing a manuscript for publication. For welding terminology, the *Welding Journal* adheres to ANSI/AWS A3.0-94, *Standard Welding Terms and Definitions.*

Papers submitted for consideration in the Welding Research Supplement are required to undergo Peer Review before acceptance for publication. Submit an original and one copy (double-spaced, with 1-in. margins on 8 ½ x 11-in. or A4 paper) of the manuscript. Submit the abstract only on a computer disk. The preferred format is from any Macintosh® word processor on a 3.5-in. double- or high-density disk. Other acceptable formats include ASCII text, Windows™ or DOS. A manuscript submission form should accompany the manuscript.

Tables and figures should be separate from the manuscript copy and only high-quality figures will be published. Figures should be original line art or glossy photos. Special instructions are required if figures are submitted by electronic means. To receive complete instructions and the manuscript submission form, please contact the Peer Review Coordinator, Doreen Kubish, at (305) 443-9353, ext. 275; FAX 305-443-7404; or write to the American Welding Society, 550 NW LeJeune Rd., Miami, FL 33126.